

# Improvement of Robot Accuracy by Calibrating Kinematic Model Using a Laser Tracking System -Compensation of Non-Geometric Errors Using Neural Networks and Selection of Optimal Measuring Points Using Genetic Algorithm-

Seiji Aoyagi, *Member, IEEE*, Atsushi Kohama, Yasutaka Nakata, Yuki Hayano, Masato Suzuki

**Abstract**—A laser tracking system is employed for measuring robot arm's tip with high accuracy. Geometric parameters in a robot kinematic model are calibrated by minimizing errors between measured positions and predicted ones based on the model. Residual errors caused by non-geometric parameters are further reduced by using neural networks, realizing high positioning accuracy of sub-millimeter order. To speed up the calibration process, the smaller number of measuring points is preferable. Optimal measuring points, which realize high positioning accuracy with small point number, are selected using genetic algorithm (GA).

## I. INTRODUCTION

At present state, almost industrial robot tasks are performed by a teaching playback method, in which a robot repeats positioning joint angles, which are taught manually in advance using a teaching pendant, etc. This method is based on comparatively high repeatability of a robot arm. The problem here is that laborious and time-consuming online manual teaching is inevitable whenever the specification of a product is changed. It is desirable to teach a task quickly to a robot manipulator when a production line and production goods are changed.

Considering these circumstances, an offline teaching based on high positioning accuracy of a robot arm is desired to take the place of the online manual teaching [1]. In the offline teaching, the joint angles to achieve a given Cartesian position of the arm's tip are calculated using a kinematic model of the robot arm. However, a nominal geometrically model according to a specification sheet does not include the errors arising in manufacturing or assembly. Moreover, it also does not include non-geometric errors, such as gear transmission errors, gear backlashes, arm compliance, etc., which are difficult to geometrically consider in a kinematic model.

Therefore, some method of calibrating precisely geometric and non-geometric parameters in a kinematic model is required, in which three dimensional (3-D) absolute position

referring to a world coordinate system should be measured [2-6]. The parameters are obtained so as that the errors between the measured positions and the predicted positions based on the kinematic model are minimized by a computer calculation using a nonlinear least square method.

In the present paper, a laser tracking system was employed for measuring the 3-D position with high accuracy of approximately 5  $\mu\text{m}$  [7-9]. As a target of calibration, a 7-DOF articulated robot was employed. After the geometric parameters were calibrated, residual errors caused by non-geometric parameters were further reduced by using neural networks (abbreviated to NN hereinafter), which is the major originality of this study.

Several researches have used NN for robot calibration. For example, it was used for interpolating the relationship between joint angles and their errors due to joint compliance in [10]. Two joints liable to suffer from gravitational torques were dealt with, and the interpolated relationships were finally incorporated into the forward kinematic model. So the role of NN was supplemental for modeling non-geometric errors. In [11], the relationship between Cartesian coordinates and positioning errors arising there was interpolated using NN. Joint angles themselves in forward kinematic model, however, were not compensated, and experimental result was limited to relative (not absolute) measurement using a calibration block in a rather narrow space. Compared with their researches, in the proposed method in this study, the joint angles in the forward kinematic model are precisely compensated using NN so as that the robot accuracy would be fairly improved in a comparatively wide area in the robot work space.

To speed up the calibration process, selecting smaller number of measuring points is preferable, while maintaining the accuracy. It is reported that the sensitivities of parameters affecting on the accuracy are desired to be averaged, i.e., not varied widely, for achieving good accuracy [12, 13]. As the index of showing the extent how sensitivities are averaged, observability index (OI) was employed [12]. Under the limitation of point number, optimal spatial selection of measuring points achieving the largest OI was investigated using genetic algorithm (GA), which is also the major originality of this study.

A. Kohama, Y. Nakata, Y. Hayano, M. Suzuki, and S. Aoyagi are with Department Mechanical Engineering, Kansai University, Suita, OSAKA 564-8680, JAPAN

(Corresponding author: Seiji Aoyagi, phone: +81-6-6368-0823; fax: +81-6-6388-8785; e-mail: aoyagi@kansai-u.ac.jp).

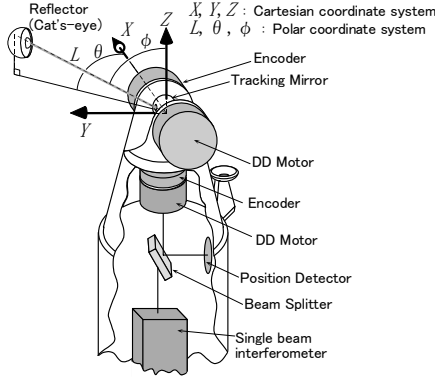


Fig. 1. Principle of measurement of SMART310

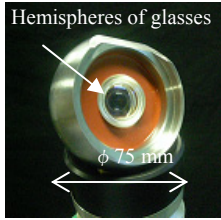


Fig. 2. Cat's-eye



Fig. 3. Experimental setup for measuring position of robot arm's tip

## II. MEASUREMENT APPARATUS FEATURING LASER TRACKING SYSTEM

Seven degrees of freedom (DOF) articulated robot (Mitsubishi Heavy Industries, product name: PA10-7C) was employed as a calibration object. A laser tracking system (Leica Co. Ltd., product name: SMART310) was used as a position measuring instrument, as shown in Fig. 1. The basic measuring principle of laser tracking system is based on that proposed by Lau [14]. A laser beam is emitted and reflected by a tracking mirror, which is installed in a reference point. Then, this beam is projected to a retro-reflector called Cat's-eye, which is fixed at the robot arm's tip as a target (see Figs. 2 and 3). The horizontal and azimuth angle of laser direction is obtained by optical encoders, which are attached to the two axes of the tracking mirror. The distance of laser path is obtained by an interferometer. Then, the position of the center of Cat's-eye, i.e., the position of robot arm's tip, can be calculated with considerably high accuracy. According to the specification sheet, this system can measure 3-D coordinates with repeatability of  $\pm 5$  ppm ( $\mu\text{m}/\text{m}$ ) and accuracy of  $\pm 10$  ppm, which are sufficient enough for the application of robot calibration.

## III. CALIBRATION OF ROBOT KINEMATIC PARAMETERS

### A. Kinematic Model Using DH parameter

The kinematic model of the robot is constructed by using Denavit-Hartenberg (DH) parameters [15]. The outline of DH notation is shown in Fig. 4. Each axis is defined as  $Z$  axis and two common perpendiculars are drawn from  $Z_{i-1}$  to  $Z_i$

and from  $Z_i$  to  $Z_{i+1}$ , respectively. The distance and the angle between these two perpendiculars are defined as  $d_i$  and  $\theta_i$ , respectively. The torsional angle between  $Z_i$  and  $Z_{i+1}$  around  $X_{i+1}$  is defined as  $\alpha_i$ . The length of the perpendicular between  $Z_i$  and  $Z_{i+1}$  is defined as  $a_i$ . Using these four parameters, the rotational and translational relationship between adjacent two links is defined. Nominal values of DH parameters of the PA10 robot on the basis of its specification sheet are shown in Table I. The deviations between the calibrated values (see the next section) and the nominal ones are also shown in this table.

The kinematic model of relationship between the measurement coordinate system (i.e., SMART310 coordinate system) and the 1st axis coordinate system of the robot is expressed by a homogeneous transformation matrix using 6 parameters (not 4 parameters of DH notation), which are 3 parameters  $\theta_x, \theta_y, \theta_z$  for expressing the rotation, and 3 parameters  $x_0, y_0, z_0$  for expressing the translation.

The kinematic model from the robot base coordinate system to the 7th joint coordinate system is calculated by the product of homogeneous coordinate transformation matrices, which includes  $4 \times 7 = 28$  DH parameters. As for the relationship between the 7th joint coordinate system and the center position of Cat's-eye, it can be expressed by using translational 3 parameters  $x_8, y_8, z_8$ . Thus, as the result, the kinematic model of the robot is expressed by using  $6+28+3 = 37$  parameters in total, which is as follows:

$$P = (x_0, y_0, z_0, \theta_x, \theta_y, \theta_z, a_1, d_1, \alpha_1, \theta_1, \dots, a_7, d_7, \alpha_7, \theta_7, x_8, y_8, z_8)^T \quad (1)$$

### B. Nonlinear Least Square Method for Calibrating Geometric Parameters

The Cat's-eye is attached to the tip of PA10 robot, and it is positioned to various points by the robot, then the 3-D

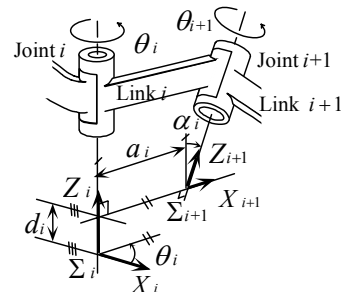


Fig. 4. DH notation

TABLE I  
DH PARAMETERS OF PA10 ROBOT

Joint	$\theta$ [deg]		$d$ [mm]		$a$ [mm]		$\alpha$ [deg]	
	Nominal value	Deviation	Nominal value	Deviation	Nominal value	Deviation	Nominal value	Deviation
1	0.0	-0.44	315.0	1.24	0.0	-0.56	-90.0	0.10
2	0.0	0.04	0.0	0.39	0.0	0.34	90.0	-0.16
3	0.0	0.57	450.0	0.96	0.0	0.32	-90.0	0.01
4	0.0	-0.15	0.0	0.35	0.0	-0.14	90.0	-0.32
5	0.0	2.12	500.0	-0.33	0.0	-0.17	-90.0	-0.52
6	0.0	0.21	0.0	0.32	0.0	0.61	90.0	-0.17
7	0.0	-1.29	80.0	-0.82	0.0	1.02	0.0	-1.25

position of robot arm's tip is measured by the laser tracking system. The parameters are obtained so that the errors between measured positions and predicted positions based on kinematic model are minimized by a computer calculation.

The concrete procedure of calibration is described as follows (also see Fig. 5): Let the joint angles be  $\Theta = (\theta_1, \theta_2, \dots, \theta_7)$ , designated Cartesian 3-D position of robot arm's tip be  $X_r = (X_r, Y_r, Z_r)$ , measured that be  $X = (X, Y, Z)$ , nominal kinematic parameters based on DH notation be  $P_n$  (see (1)). Then, the nominal forward kinematic model based on the specification sheet is expressed as  $X = f(\Theta, P_n)$ .

By using the nominal kinematic model, the joint angle  $\Theta_r$  to realize  $X_r$  are calculated, i.e., the inverse kinematic is solved, which is expressed in the mathematical form as  $\Theta_r = f^{-1}(X_r, P_n)$ .

The joint angles are positioned to  $\Theta_r$ , then, the 3-D position of robot arm's tip is measured as  $X$ . Let the calibrated parameters be  $\hat{P}$ , and the predicted position based on the calibrated model be  $\hat{X}$ , then the forward kinematic model using them is expressed as  $\hat{X} = f(\Theta_r, \hat{P})$ . The  $\hat{P}$  is obtained so that the sum of the errors between the measured positions  $X$  and the predicted positions  $\hat{X}$  is minimized by using a nonlinear least square method.

#### C. Method I -Modeling of Non-Geometric Errors-

Referring to other researches [3, 4], typical non-geometric errors of gear transmission errors and joint compliance are modeled herein, for the comparison with the method using NN proposed in this study, the detail of which is explained in the next Section III.D.

It is considered that the gear transmission error of  $\theta^{gt}$  arises from the eccentricity of each reduction gear. This error is expressed by summation of sinusoidal curve with one period and that with  $n$  periods as follows:

$$\Delta\theta_i^{gt} = P_{i1}^{gt} \sin(\alpha_i + \phi_{i1}) + P_{i2}^{gt} \sin(n_i\alpha_i + \phi_{i2}), \quad (2)$$

where  $i$  is joint number ( $1 \leq i \leq 7$ ),  $\alpha_i$  is the joint angle detected by a rotary encoder sensor,  $n_i$  is the reduction ratio,  $P_{i1}^{gt}$ ,  $P_{i2}^{gt}$ ,  $\phi_{i1}$ ,  $\phi_{i2}$  are parameters to be calibrated.

As for the joint no. 2 and no. 4, which largely suffer from torques caused by arm weights, the joint angle errors of  $\Delta\theta_2^{con}$  and  $\Delta\theta_4^{con}$  due to joint compliances are expressed as

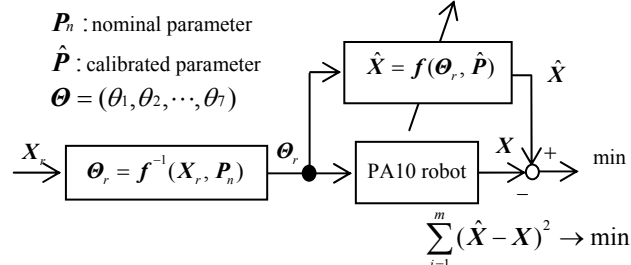


Fig. 5. Calibration procedure by nonlinear least square method

follows:

$$\Delta\theta_2^{con} = P_1^{con} \sin \alpha_2 + P_2^{con} \sin(\alpha_2 + \alpha_4), \quad (3)$$

$$\Delta\theta_4^{con} = P_3^{con} \sin(\alpha_2 + \alpha_4), \quad (4)$$

where  $P_1^{con}$ ,  $P_2^{con}$ ,  $P_3^{con}$  are parameters to be calibrated.

In a forward kinematic model,  $\theta_i$  is dealt with as follows:  $\theta_i = \alpha_i + \Delta\theta_i^{gt}$  ( $i = 1, 3, 5, 6, 7$ ),  $\theta_i = \alpha_i + \Delta\theta_i^{gt} + \Delta\theta_i^{con}$  ( $i = 2, 4$ ). As the parameters,  $P_{i1}^{gt}$ ,  $P_{i2}^{gt}$ ,  $\phi_{i1}$ ,  $\phi_{i2}$  ( $0 \leq i \leq 7$ ),  $P_1^{con}$ ,  $P_2^{con}$ ,  $P_3^{con}$  are added to  $P$  in (1), forming 68 parameters in total.

#### D. Method II -Using Neural Networks for Compensating Non-Geometric Errors-

Non-geometric errors have severely nonlinear characteristics as shown in (2)-(4). Therefore, a method is proposed herein as follows: after the geometric parameters are calibrated, the residual errors caused by non-geometric parameters are further reduced by using NN, considering that NN gives an appropriate solution for a nonlinear problem.

The concrete procedure using NN is described as follows (also see Fig. 6): Typical three layered forward type NN was applied. The input layer is composed of 3 units, which correspond to Cartesian coordinates of  $X$ ,  $Y$ , and  $Z$ . The hidden layer is composed of 100 units. The output layer is composed of 7 units, which correspond to compensation values of 7 joint angles, which is expressed as  $\Delta\hat{\Theta}_p = (\Delta\hat{\theta}_1, \Delta\hat{\theta}_2, \dots, \Delta\hat{\theta}_7)$  and is added to the  $\Theta$  parameter in DH model.

In the learning of NN, measured data of robot arm's tip  $X = (X, Y, Z)$  is adopted as the input data to NN. Then, the parameter  $\Delta\hat{\Theta}_p$  to satisfy  $X = f(\hat{\Theta}_r, \hat{P} + \Delta\hat{\Theta}_p)$  is calculated numerically by a nonlinear least square method, where  $\hat{\Theta}_r = f^{-1}(X_r, \hat{P})$  is the joint angle to realize  $X_r$  based on the kinematic model using calibrated parameters  $\hat{P}$  (see the previous Section III.B).

Then, the obtained many of pairs of  $(X, \Delta\hat{\Theta}_p)$  are used as

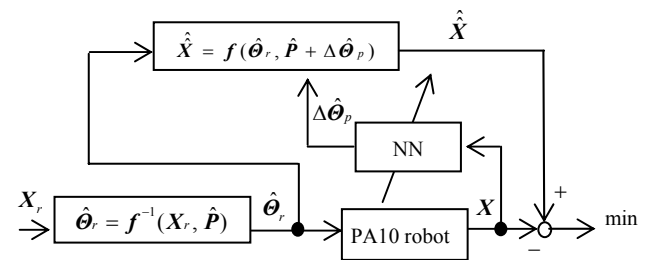


Fig.6. Learning procedure of NN

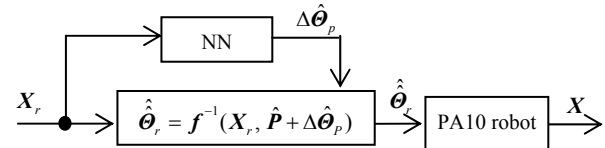


Fig.7. Implementation of NN

the teaching data for NN learning, in which the connecting weights between units, i.e., neurons, are calculated. For this numerical calculation, RPROP algorithm [16], which modifies the conventional back-propagation method, is employed.

#### E. Implementation of Neural Networks for Practical Robot Positioning

Figure 7 shows the implementation of NN for practical robot positioning. When  $X_r$  is given, the compensation parameter  $\Delta\hat{\theta}_p$  is obtained by using NN, then, the accurate kinematic model including  $\Delta\hat{\theta}_p$  is constructed. Using this model, the joint angle  $\hat{\theta}_r = f^{-1}(X_r, \hat{P} + \Delta\hat{\theta}_p)$  is calculated numerically, and it is positioned by a robot controller. Then,  $X_r$  is ideally realized.

### IV. EXPERIMENTAL RESULTS OF CALIBRATION

#### A. Group of Points for Teaching and Verification

Measurement area of  $400 \times 400 \times 300$  mm was set, as shown in Fig. 8. This area was divided at intervals of 100 mm for  $x$ ,  $y$ , and  $z$  coordinates. As the result,  $5 \times 5 \times 4 = 100$  grid points were generated. The group of the grid points was used for teaching set for calibration.

On the other hand, the group of 100 points were taken as shown in Fig. 9, which are located at regular intervals on a circular path, of which radius is 100 mm and center is (500, 100, 600) mm. They were used for verification set for the calibration result.

#### B. Results of Verification of Calibrated Model

The joint angles to realize the verification set were calculated based on the calibrated model, and they were positioned by a robot controller. Note that, this calculation of inverse kinematics is not solved analytically, so it should be numerically solved, since the adjacent joint axes in the calibrated model are no longer accurately parallel or perpendicular to each other.

Then, the Cartesian 3-D positions of the robot arm's tip, i.e., the verification set, were measured by the laser tracking system. By comparing the measured data with the designated data, the validity of the calibrated kinematic model was estimated.

Figure 10 and Table II show the results in the first trial (called Trial 1). In this figure, error means the norm of  $\sqrt{(X - X_r)^2 + (Y - Y_r)^2 + (Z - Z_r)^2}$ . This definition is valid for the following of this article.

#### C. Discussion (Comparison between Method I -Modeling of Non-Geometric Errors- and Method II -Using Neural Networks for Compensating Non-Geometric Errors-)

It was proven that the error was drastically reduced from 5.2 mm to 0.29 mm by calibrating geometric parameters using a nonlinear least square method. It was proven that the error was further reduced to 0.19 mm by compensating

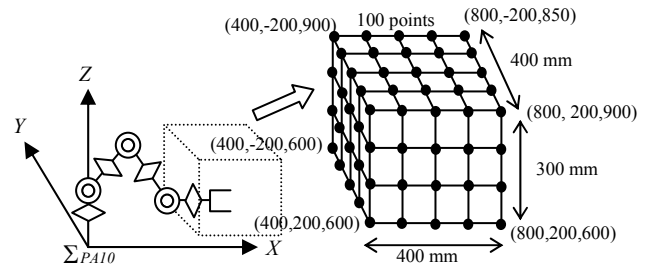


Fig.8. Measurement points for teaching data set

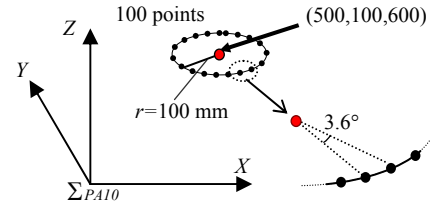


Fig.9. Measurement points for verification data set

non-geometric parameters using NN, indicating effectiveness of Method II.

The error was reduced by calibrating both geometric and non-geometric parameters using a nonlinear least square method, i.e., by applying Method I. The improvement from calibrating only the geometric parameters (not non-geometric parameters) using a nonlinear least square method, however, was subtle and incremental, which was from 0.29 to 0.24 mm.

To verify that the experimental result is repeatable, the

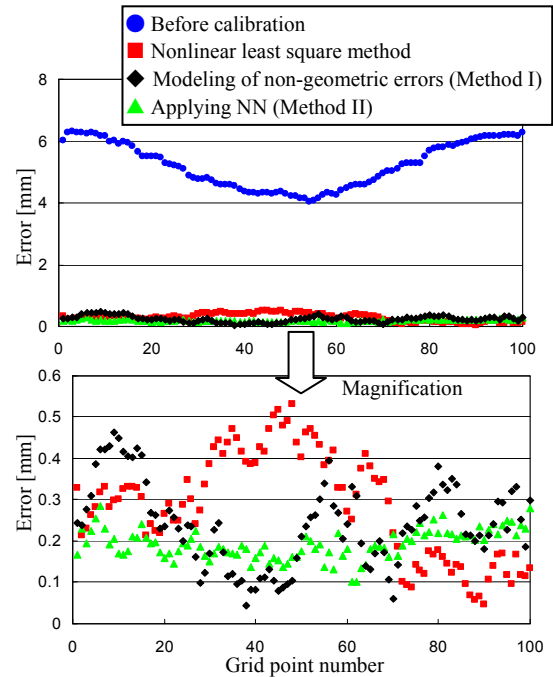


Fig.10. Result at points for verification

TABLE II

AVERAGE OF ERRORS IN POINTS FOR VERIFICATION (unit: mm)

	Trial 1	Trial 2	Trial 3
Before calibration	5.23	8.37	7.86
Nonlinear least square method	0.29	0.35	0.33
Modeling of non-geometric errors (Method I)	0.24	0.26	0.27
Applying NN (Method II)	0.19	0.17	0.15

calibration process was carried out again for the same verification data set on the same circular path, called Trial 2. And it was carried out for data set on another circular path, of which  $z$  coordinate is shifted from original 600 to 700 mm, called Trial 3. These results are added and shown in Table II. Compared Trials 2 and 3 with Trial 1, it is proven that the experimental trend of average errors is repeatable.

Eventually, it is proven that Method II of first calibrating the geometric parameters and next further compensating the non-geometric parameters using NN is the best among these procedures. The reason of superiority of Method II is thought to be as follows: there are many unexpected non-geometric errors besides the gear transmission errors and joint compliances. Therefore, Method I of only considering these two type non-geometric errors did not work so well. On the other hand, NN can compensate all types of non-geometric errors by imposing the resultant errors in its learning process appropriately to the variety of connecting-weights of neurons.

Even in case of using NN, there remain still positioning errors of approximately 0.2 mm. They supposedly arise from the limitation of generalization ability of NN, since the points for verification are considerably apart from those for teaching.

## V. SELECTION OF OPTIMAL MEASURING POINTS USING GENETIC ALGORITHM (GA)

### A. Meaning of Reducing the Number of Measuring Points

For shortening the time required for the calibration process, reducing the number of measuring points while maintaining the accuracy is effective. For increasing calibration accuracy, it is important that the sensitivity of (tip position displacement)/(parameter fluctuation) is uniform for all the parameters in a kinematic model. As the index of showing the extent how the sensitivity is uniform among the parameters, observability index (OI) was reported [12]. The larger OI means the higher uniformity. In this section, under the limitation of point number, optimal spatial selection of measuring points achieving the largest OI is investigated using genetic algorithm (GA).

The procedure of obtaining OI is described hereinafter. Let the forward kinematic model be  $\mathbf{X} = \mathbf{f}(\boldsymbol{\Theta}, \mathbf{P})$ , as already explained in Section III.B. Then, the error of robot arm's tip  $\Delta \mathbf{X}$  with respect to the error of geometric parameters  $\Delta \mathbf{P}$  is expressed as follows:

$$\Delta \mathbf{X} = \frac{\partial \mathbf{X}}{\partial \mathbf{P}} \Delta \mathbf{P} = \mathbf{J} \Delta \mathbf{P}, \quad (5)$$

where  $\mathbf{J}(3 \times n)$  is the Jacobian matrix,  $n$  is the number of geometric parameters. Assuming the number of measuring points be  $m$ , equation (5) is extended as follows:

$$\Delta \mathbf{Y} = \mathbf{B} \Delta \mathbf{P}, \quad (6)$$

where  $\Delta \mathbf{Y} = [\Delta \mathbf{X}_1^T, \Delta \mathbf{X}_2^T, \dots, \Delta \mathbf{X}_m^T]^T$  ( $3m \times 1$ ), and

$\mathbf{B} = [\mathbf{J}_1^T, \mathbf{J}_2^T, \dots, \mathbf{J}_m^T]^T$  ( $3m \times n$ ). By applying singular value decomposition to the extended Jacobian matrix  $\mathbf{B}$ , singular values  $\sigma_1 \sim \sigma_n$  are obtained, which are equivalent to the sensitivities of geometric parameters  $p_1 \sim p_n$ , respectively. By using  $\sigma_1 \sim \sigma_n$ , OI is defined as follows:

$$\text{OI} = \frac{\sqrt[n]{\sigma_1 \sigma_2 \dots \sigma_n}}{\sqrt{m}}. \quad (7)$$

### B. Selection of Optimal Measuring Points Using GA

It is impossible to analytically define the optimal measuring points that maximize OI. Therefore, GA was applied, which is known as an effective method for searching an optimal (or nearly optimal) solution of a severely nonlinear problem.

The procedure of pursuing the optimal spatial selection of measuring points is described hereinafter. Let us assume that the number of measuring points is limited to 8, for example. Then, a chromosome is provided, which consists of  $X$ ,  $Y$ , and  $Z$  coordinates of 8 points. As 8 bit is assigned to each coordinate, the chromosome consists of totally 8 points  $\times$  3 coordinates  $\times$  8 bit = 192 bit, as shown in Fig. 11.

Note that the 14 singular values were almost zero; therefore the effective (not-redundant) number of singular values [13] is  $37-14=23$ . Three equations are obtained for  $X$ ,  $Y$ , and  $Z$  coordinates at each point measurement, so the minimum number of measurement points is 8, since  $23/3=7.67$ .

Six chromosomes are randomly employed at first. By repeating crossover and mutation at each generation with referring to the fitness function of OI, they are finally converged to such a chromosome that realizes the largest OI.

### C. Experimental Results

At several numbers of generations, GA search was stopped, and the resultant 8 measuring points and corresponding OI were checked. At these 8 points, the robot arm's tip was measured by the laser tracking system. Using the measured

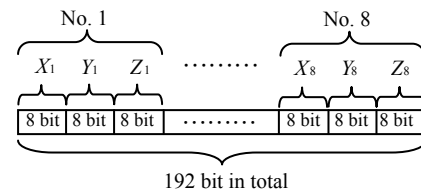


Fig. 11. Chromosome of GA

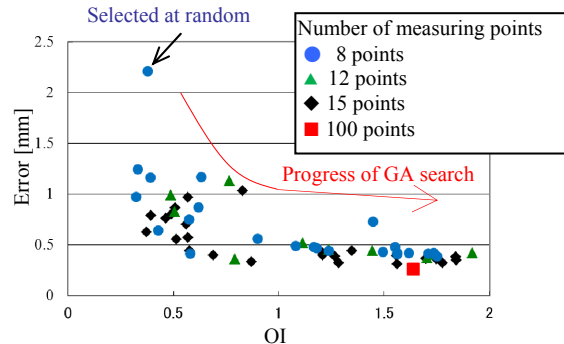


Fig. 12. Relationship between OI and positioning error

data, the kinematic model was calibrated by a nonlinear least square method. Then, based on the calibrated kinematic model, the robot arm's tip was positioned to 100 points for verification, where the absolute error was estimated again by the laser tracking system. These procedures were repeated during the progress of GA search.

The resultant relationship between OI and the positioning error is shown in Fig. 12. At first, the 8 points were selected at random, then, the GA search progresses, finally it is truncated when the number of generation reaches 1,000. From this figure, it is proven that OI is increased and the resultant error is reduced as the GA search progresses.

The data in cases that the number of measuring points is 12 and 15 are also shown in this figure. In these cases, the resultant error is less dependent on OI value, indicating that the random selection of 15 points is rather possible for maintaining the accuracy. It is supposedly because the number of measuring points is enough compared with minimum 8 points. For reference, OI of 100 points in teaching points shown in Fig. 8, and the resultant error using these points, are also depicted in this figure. It indicates that 100 points are not necessary and even 8 points are enough if they are optimally selected.

Figure 13 shows an example of 8 measuring points, which were selected by the GA search. The resultant OI for these 8 points is 1.75. For the reference, randomly selected 8 points at the beginning of the GA search are also shown in this figure, the OI for which is 0.3. Looking at this figure, measuring points with larger OI are distributed widely in the 3D space, whereas those with smaller OI are gathered in a comparatively small area.

## VI. CONCLUSIONS

A laser tracking system is employed for measuring the robot arm's tip with high accuracy. By using the measured data, the kinematic model of the robot arm is calibrated, and the high positioning accuracy within 0.3 mm is realized.

To briefly summarize, 1) the geometric parameters are calibrated by minimizing errors between the measured positions and the predicted ones based on the kinematic model. 2) The residual errors mainly caused by non-geometric parameters are further reduced using neural networks. 3) Optimal measuring points, which realize high positioning accuracy with small point number, are selected using genetic algorithm (GA).

If the orientation of robot arm's tip could be precisely measured using some sensor such as a gyroscope [9], the robot kinematic model of realizing both position and orientation can be calibrated, which is planned to do in a future projected work.

## REFERENCES

[1] B. W. Mooring, Z. S. Roth, and M. R. Driels, *Fundamentals of Manipulator Calibration*, New York: Wiley & Sons, 1991.  
 [2] B. W. Mooring and S. S. Padavala, "The Effect of Kinematic Model Complexity on Manipulator Accuracy," in *Proc. IEEE Int. Conf. Robotics and Automation*, pp. 593-598, 1989.

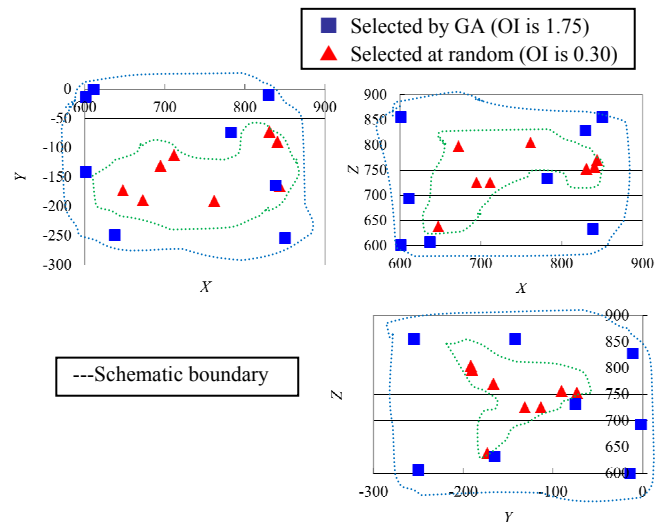


Fig. 13. Distribution of selected measuring points

[3] D. E. Whitney, C. A. Lozinski, and J. M. Rourke, "Industrial Robot Forward Calibration Method and Results," *J. Dyn. Syst. Meas. Contr.*, vol. 108, no. 1, pp. 1-8, 1986.  
 [4] R. P. Judd and A. B. Knasinski, "A Technique to Calibrate Industrial Robots with Experimental Verification," *IEEE Trans. Robotics and Automation*, vol. 6, no. 1, pp. 20-30, 1990.  
 [5] H. W. Stone, *Kinematic Modeling, Identification, and Control of Robotic Manipulators*, Norwell, Mass.: Kluwer Academic Publishers, 1987.  
 [6] S. Komai and S. Aoyagi, "Calibration of Kinematic Parameters of a Robot Using Neural Networks by a Motion Capture System," in *Proc. Annual Spring Meeting The JSPE*, pp. 1151-1152, 2007 (in Japanese).  
 [7] Y. Koseki, T. Arai, K. Sugimoto, T. Takatsuji, and M. Goto, "Accuracy Evaluation of Parallel Mechanism Using Laser Tracking Coordinate Measuring System," *J. Society of Instrument and Control Engineers*, vol. 34, no. 7, pp. 726-733, 1998 (in Japanese).  
 [8] J. Fujioka, S. Aoyagi, K. Ishii, H. Seki, and Y. Kamiya, "Study on Robot Calibration Using a Laser Tracking System (2nd Report) -Discussion on How to Select Parameters, Number of Measurement and Pose of Measurement in Multiple Positioning Method-," *J. The Japan Society for Precision Engineering*, vol. 67, no. 4, pp. 676-682, 2001 (in Japanese).  
 [9] J. Fujioka, S. Aoyagi, H. Seki, and Y. Kamiya, "Development of Orientation Measuring System of a Robot Using a Gyroscope (2nd Report) -Proposal of Position and Orientation Calibration Method of a Robot Using Both Laser Tracking System and Gyroscope-," *J. The Japan Society for Precision Engineering*, vol. 67, no. 10, pp. 1657-1663, 2001 (in Japanese).  
 [10] J. H. Jang, S. H. Kim, and Y. K. Kwak, "Calibration of Geometric and Non-Geometric Errors of an Industrial Robot," *Robotica*, vol. 19, pp. 311-321, 2001.  
 [11] K. Maekawa, "Calibration for High accuracy of Positioning by Neural Networks," *J. Robotics Society of Japan*, vol. 13, no. 7, pp. 35-36, 1995 (in Japanese).  
 [12] J. Borm and C. Menq, "Determination of Optimal Measurement Configurations for Robot Calibration Based on Observability Measure," *The Int. J. Robotics Research*, vol. 10, no. 1, pp. 51-63, 1991.  
 [13] M. Ishii, S. Sakane, M. Kakikura, and Y. Mikami, "Robot Manipulator Calibration for 3D Model Based Robot systems," *J. Robotics Society of Japan*, vol. 7, no. 2, pp. 74-83, 1988 (in Japanese).  
 [14] K. Lau, R. J. Hocken, and W. C. Haight, "Automatic Laser Tracking Interferometer System for Robot Metrology, Precision Engineering," vol. 8, no. 1, pp. 3-8, 1986.  
 [15] J. Denavit and R. S. Hartenberg, "A Kinematic Notation for Lower Pair Mechanism Based on Matrices," *ASME J. Applied Mechanics*, pp. 215-221, 1955.  
 [16] M. Riedmiller and H. Braun, "A Direct Adaptive Method for Faster Backpropagation Learning: The RPROP Algorithm," in *Proc. IEEE Int. Conf. Neural Networks*, pp. 586-591, 1993.